P 9.4 Assimilation of radar observations in mesoscale models using approximate background error covariance matrices

Chang-Hwan Park, Mark S. Kulie, and Ralf Bennartz*
Atmospheric and Oceanic Sciences, University of Wisconsin – Madison

1) Introduction

Forecasting severe thunderstorms and convective systems plays an important role in weather prediction. Severe thunderstorms can develop very quickly and can produce high winds, hail, and flash flooding, which are potentially life-threatening and can cause substantial property damage in a short time. According to the U.S. Natural Hazard Statistics over 30 year average (1977-2006), "Flash floods/floods are the #1 cause of deaths associated with thunderstorms." (Sky warn review by Phil Hysell). Also, NOAA's annual compilations of flood loss statistics show that the damage scale of the flood tends to increase with time, possibly mostly due to urban spread. Fast and accurate nowcasting and short-term forecasting systems, including the prediction of timing, location, and intensity of the severe storm, are becoming more and more important in this regard.

Mesoscale models together with advanced methods to incorporate radar and other real-time observations have become one increasingly popular research venue in this area. Only radars allow for observing convective scale thunderstorms at high temporal and spatial resolution (Sun 2005). The rapid evolution of mesoscale systems as well as the non-linear relation between radar reflectivity and precipitation intensity makes the assimilation of radar data into models a challenging problem, both mathematically and physically.

Specifically, problems include the non-linearity of the observation operator (Evensen 2003), non-Gaussian background errors (Harlim and Hunt 2007), filter divergence (Houtekamer and Mitchell 1998), as well as the flow-dependence of the background-error covariances (Houtekamer and Mitchell 1998; Houtekamer and Mitchell 2001; Houtekamer, Mitchell et al. 2005).

*Corresponding author address: Ralf Bennartz, University of Wisconsin-Madison, Atmospheric & Oceanic Science Dept. WI
e-mail: bennartz@aos.wisc.edu

2) New Methods

a) *HA approximation*

The matrix **HA** can be interpreted as the deviation of the ensemble members from the ensemble mean state mapped into observation space. The crucial assumption underlying the matrix **HA** is that the observation operator can be approximated by a linear function around the mean state. This means that the ensemble spread response of the observation operator to the model variables is supposed to be linear. This requires the deviations between the individual ensemble members and the mean state to be small, an assumption which is frequently violated when dealing with, for example, intermittent phenomena such as clouds and precipitation. Furthermore, when dealing with strongly non-linear observation operators, the distribution of HA will most likely not be Gaussian, even if A is Gaussian. The impact of a non-linear observation operator is schematically depicted in Fig. 1. The strongly non-linear observation operator in Fig.1-c will map all negative distributions of the model PDF onto zero in observation space and create a highly skewed PDF in observation space. This is a common problem with radar observations.

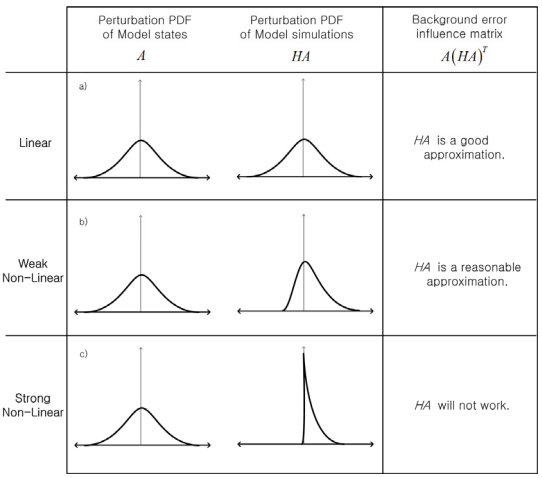

Fig. 1. Schematic distribution types of observation operators perturbation simulated after

perturbation of model states a) linear observation operator forming a Gaussian distribution b) weakly non-linear observation operator forming a skewed Gaussian distribution c) strongly non-linear observation operator forming a highly non-Gaussian distribution

The assimilation of intermittent observations might also lead to rank-deficiencies in **B,** for example, in cases where neither of the ensemble members produces precipitation.

Assume an observable variable is linked to the state of the model via a strongly non-linear forward operator, such as precipitation rate. In this case **HA** represents the deviation of the individual ensemble members from the ensemble mean. Since the distribution of precipitation rate is typically highly skewed, the resulting distribution of **HA** will be highly skewed and not well suited for assimilation purposes. While precipitation rate is observed, the underlying process (e.g. 'convection triggering precipitation') might not be observed directly. However, various other model variables will be correlated with this process. For a typical convective precipitation situation, deviations in temperature in the boundary layer might be positively correlated with deviations in precipitation. In this paper, a new method is proposed to address this issue. The basic idea relies on the aforementioned correlative model variables and can be put into very simple terms:

'If the background error correlation in observation space cannot be used directly, it might be approximated by another variable, which is correlated with the observations and has better error characteristics.'

This method corresponds to a translation of the non-Gaussian PDF into a Gaussian form, maintaining its original physical units. In Fig.2, the process is schematically explained. Two variables are shown as observable variable *y* and observation proxy *Y*. The PDF of the observable variables y forms shows a non-Gaussian distribution (blue curve) whereas the observation proxy *Y* (red curve) has a Gaussian distribution and the positive part of the distribution is well correlated to observable *y*.

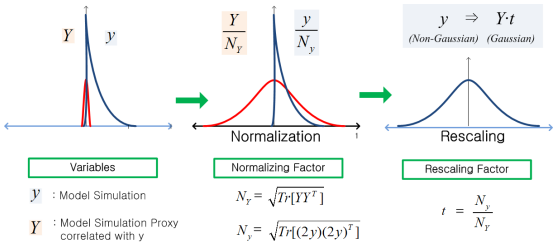

Fig. 2. New method in general from : Modulation of Probability Density Function (PDF) between different physical variables by normalization process with rescaling factors

The proxy background error covariance in observation space can now be derived via a rescaling. The ratio of the traces of the original background error covariance and the proxy are used to renormalize the total variance of the approximated background error covariance to match the physical units of **R** in the subsequent EnKF calculations. Note that the ratio of the traces of these matrices is only a scalar factor and other, more sophisticated methods might be devised in addition.

Another issue related to ensemble assimilation is the triggering of clouds or precipitation in cases where initially none of the ensemble members produce any cloud or precipitation. In such cases *HA* collapses to identical zero and no assimilation can be performed. Replacing *HA* with a proxy variable will yield a well-defined background error covariance and potentially will allow conditions favorable to clouds or precipitation in the assimilation. This is highlighted in Fig. 2, middle panel. Assume the PDF of precipitation (blue curve) to be approximated by an ensemble with all identical zeros. Then the background error covariance will collapse. Assume the red curve to be the distribution of potential temperature in the boundary layer. Areas with high potential temperature will correspond to high precipitation and areas with lower potential temperature to zero precipitation. By replacing the black with the red curve, a better proxy of the true error covariance will be obtained.

Using the variable A_o to denominate the proxy for *HA*, this leads to the following approximation for *HA* in the Kalman gain:

$$HA \approx A_o \cdot t \qquad (1)$$

The revised Kalman gain can now be expressed as:

$$K = \left(\frac{1}{s-1} A A_o^T t\right)\left(\frac{1}{s-1} A_o A_o^T t^2 + R\right)^{-1} \quad (2)$$

The rescaling factor t allows us to translate HA into A_o maintaining the units of the observation space. The next step is to find a suitable proxy for HA. This proxy can for example be part of the ensemble itself as long as certain criteria are fulfilled. A variable needs to be picked, which is well correlated with the model simulation HA. In the present study, we use potential temperature deviations in the boundary layer, which are well correlated with the initiation of convective precipitation. The Kalman gain can be slightly reformulated to gain insight into the data assimilation process. When we extract the background error covariance matrix from the background error influence term by placing an imaginary $HBH^T \cdot (HBH^T)^{-1}$ between the two terms in brackets in Eq. (2) we can rewrite the Kalman gain as:

$$K = \underbrace{AA_o^T \left(A_o A_o^T\right)^{-1}}_{\text{Response information}} \cdot \underbrace{\left(I + R \cdot B_o^{-1} t^{-2}\right)^{-1}}_{\text{Error information}} \cdot \underbrace{t^{-1}}_{\text{Rescalering}} \quad (3)$$

This reformulation allows us to clearly see the response information and the error information between the background state and the observation. The possible situations in the data assimilation study are presented in Table 1.

Table 1 : The influence of the background and the observation errors on the observation assimilation

C	Error Norms	Error Information N in K	Observation Update $K(D-HX)$
1	$\|R\| << \|B_o t^2\|$	I	Large-update
2	$\|R\| \approx \|B_o t^2\|$	$2 \cdot I$	Intermediate-update
3	$\|R\| > \|B_o t^2\|$	Large	Small-update
4	$\|R\| >> \|B_o t^2\|$	Very Large	Non-update

b) Background Error renormalization

Due to the different temporal error evolution, the magnitude of the background error can be underestimated compared to the observation error in the data assimilation. This problem is schematically illustrated in the Fig. 3.

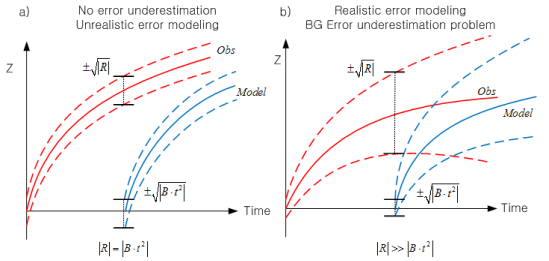

Fig. 3. Background error underestimation problem a) absolute error simulation, b) relative error simulation (interval indication in blue curves - BG error in the convective initiation stage, in red curves - OB error in developing stage)

Due to the non-linear relationship in the perturbation process, the range interval of the blue lines, HA, in Fig. 3 would be intensified nonlinearly with time, even though the perturbation A maintains the constant interval over the whole cycle. The observation error R is also not constant as a relative error which is proportional to the true state variation. Therefore, the constant absolute error shown in Fig. 3-a is an unrealistic error simulation regardless of not having the underestimation problem of the BG error. On the other hand, with the realistic error modeling (Fig. 3-b), the underestimation of the BG error is an inevitable problem in the data assimilation. For example, in the Madison flood case study, it is found that the model simulation produced the initial precipitation approximately 1 hour later than the KMKX radar measurement. This time difference causes the Kalman filter consistently to ignore the well quality-controlled and highly resolved radar observation during assimilation cycles. Consequently the radar data assimilation by EnKF couldn't improve the forecast results. Therefore, the next step of the new method is the weighting technique to take into account this temporal evolution of the different error sources in the data assimilation.

weighting to BGE covariance matix

$$BH^T \Rightarrow (2-f) \cdot BH^T$$

$$= \frac{1}{s-1}\left(\sqrt{2-f}\, A\right)\left(\sqrt{2-f}\, A_o \cdot t\right)^T \quad \textbf{(4)}$$

$$HBH^T \Rightarrow (2-f) \cdot HBH^T$$

$$= \frac{1}{s-1}\left(\sqrt{2-f}\, A_o \cdot t\right)\left(\sqrt{2-f}\, A_o \cdot t\right)^T$$

weighting to OBE covariance matix

$$R \Rightarrow f \cdot R \quad \textbf{(5)}$$

The weighting factor f linearly modulates the magnitude of observation and background errors (See Eq.(4) and (5)).

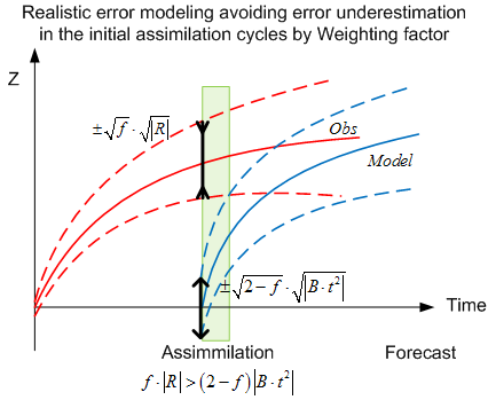

Fig. 4. Weighting factor for the OB error and the underestimated BG error to improve the update process in the data assimilation cycles

In the assimilation cycles the observation error is the more evolved state than the background model error in this study. Therefore, the f in Fig. 4 is chosen as less than 1 to reduce the difference between OB and BG errors. It means that by the weighting technique the C.4 in the Table. 1 can change into C.3 allowing the effective update through the multiple assimilation cycles without an abrupt model imbalance which can happen in C.1 and C.2. The weighting term can be simplified in EnKF formulation as following expression.

$$K = \underbrace{AA_o^T\left(A_oA_o^T\right)^{-1}}_{\text{Response Information}}\cdot\underbrace{\left(I+\frac{f}{2-f}\cdot R\cdot B_o^{-1}t^{-2}\right)^{-1}}_{\text{Renormalized Error Information}}\cdot\underbrace{t^{-1}}_{\text{rescaling}} \quad (6)$$

This expression tells us that the introduced weighting technique adjusts only the relative error ratio ($R\cdot B^{-1}t^{-2}$) in the error normalization term, maintaining the ensemble sizes of A and HA (A_ot in the new method) in the observation influence term. It means that this modification only renormalizes the observation increment. This method basically resolves all kinds of inactive update problems due to the BG error underestimation caused by the insufficiently perturbed ensemble spread, the filter divergence and the time lag between the BG and OB errors in the data assimilation process.

In the expression of Sherman–Morrison–Woodbury formula to reduce computational expense when dealing with a large number of data points (Mandel 2006), the final Kalman gain in EnKF with weighting factor and rescaling factor is derived as,

$$\tilde{K} = K\cdot t$$
$$= \kappa\cdot AA_o^TR^{-1}\left[I-\kappa\cdot A_o\left(I+\kappa\cdot A_o^TR^{-1}A_o\right)^{-1}A_o^TR_o^{-1}\right]$$

$$\text{Where}\quad \kappa = \frac{2-f}{f\cdot t\cdot(s-1)} \qquad (7)$$

This newly expressed Kalman gain $\tilde{K}$ is non-dimensional. Also, all factors in $\tilde{K}$ are incorporated into just one constant, κ.

After applying the new method, the full expression of approximate EnKF for the highly non-linear case is

$$\hat{X} = X+\tilde{K}\left(D-HX\right)/t \qquad (8)$$

3) Results and Analysis

a) Filter Stabilization and Forecast Correlation by the HA approximation

The HA approximation includes two important considerations: the Gaussian form in HA for the stable recursive filter assimilation and the proper forecast correlation information for the forecast improvement. Firstly, the EnKF with the non-linear observation operator suffers from the unstable filter update process. For instance, the non-Gaussian *HA* (Fig. 5-a in EXP.1) due to the non-linearity between *HA-A* creates the skewed spread update at 1630 UTC (Fig. 5-b in EXP.1). By the recursive filter process, the spread update term at 1645UTC produces unrealistically significant θ indicating over 100 Kelvin (□- profile in Fig. 5 -c). Also, the *K* loses the consistent filter controllability showing different spread update patterns at 1630 and 1645 UTC (compare the □- profile in Fig. 5 b and c). On the other hand, when we look at the EXP.2 in the Fig. 5, the data assimilation by EnKF with the approximate *HA* consistently maintains the Gaussian distribution at 1630UTC and 1645UTC; during the recursive filter updates the data assimilation is

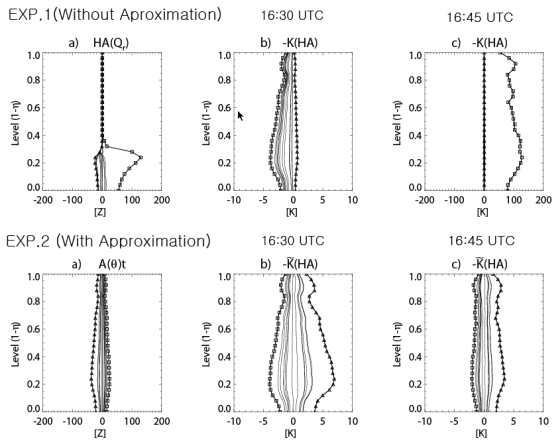

Fig. 5. Filter Stabilization test: EXP.1 (without *HA* approximation): a) Original HA (radar reflectivity, Z), b) Non-Gaussian spread update at 1630UTC (potential temperature, Kelvin), c) Non-Gaussian spread update at 1645UTC, EXP.2 (with *HA* approximation): a) Approximate HA , b) Gaussian spread update at 1630UTC, c) Gaussian spread update at 1645UTC

The second problem is the inappropriate forecast correlation between *HA* and *A*. The cause of the Madison flood is the potential instability. It means that the positively perturbed ensemble member in the current *A*(θ) (high potential instability) will create the positive ensemble member in the future *HA*(Qr) (high convective precipitation). Therefore, in this study the negative instant correlation (condensation tendency) of the original *K* is replaced with the positive forecast correlation (convective tendency), by selecting the *HA* proxy which is positively correlated with *A*. Based on this *HA-A* relationship, the positive input innovation *(D-HX)* is assimilated to increase θ in the current model state (reds curves after spin-up in Fig. 6-b) and produces the large Qr forecast improvements (reds curves after spin-up in Fig. 6-c).

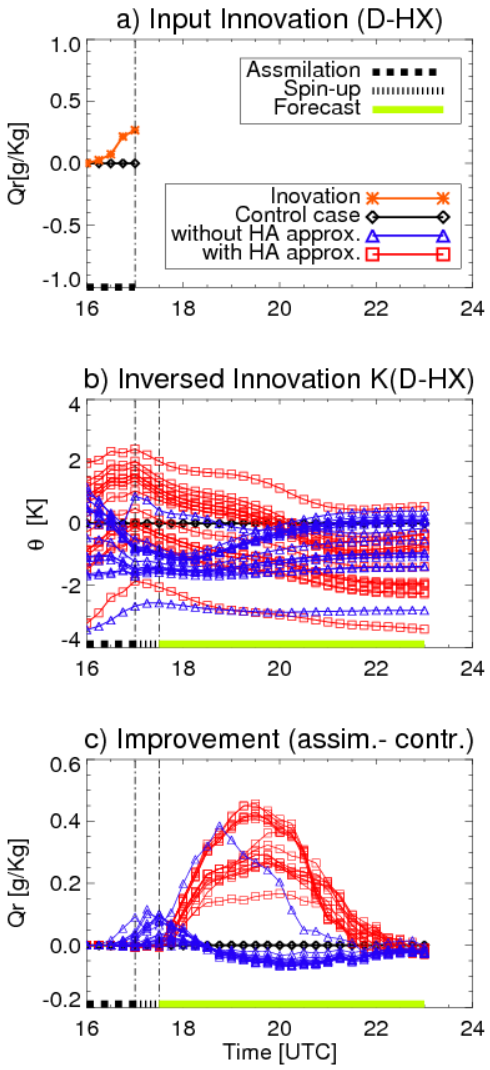

Fig. 6. Forecast Correlation test : a) Positive Innovation based on higher observation and lower current model state, b) Inversed Innovation controlled by correlation and error information of K, c) Improved forecast by input innovation, (EXP.1 : blue – no approximation with f=1.999, EXP.3 : red - approximation with f=0.1)

b) Renormalization of the error information by the Weighting technique

Another important feature of the new method is the error renormalization by the weighting technique. The results of the weighting experiments are examined on three temporal stages. The forecast model modification by radar observations communicates the potential instability. For instance, from 1600UTC to 1700UTC the observation innovations renormalized by the various weighting factors are assimilated into the WRF model as the

different ensemble mean increases in the θ field at the surface layer (Fig.7-a). According to the perturbation method, the ensemble member with increased θ contains the greater potential instability.

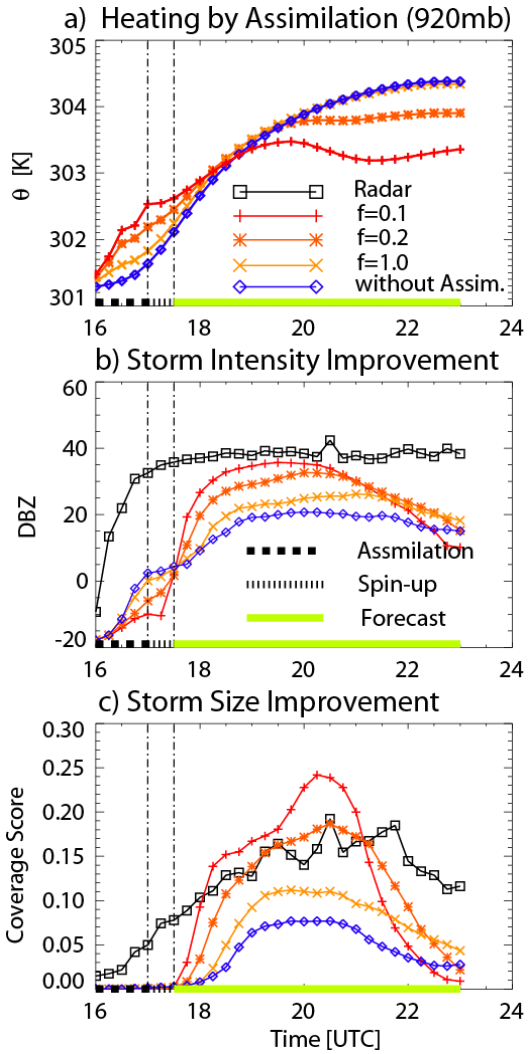

Fig. 7. Error weighting test: a) the updated model stated by the inversed innovation b) the mean reflectivity intensity improvements according to various weighting factors, c) Storm Coverage distribution improvement with the threshold value 10 dBZ for the meaningful storm scale precipitation excluding unrealistic bubble feature.)

Therefore, the overall θ growth by the radar data assimilation (the mean θ increase in Fig.7-a) represent that ensemble forecast model is improved with an increased potential instability. Then the enhanced potential instability initiates deep convections after spin-up cycles. Though, the spin-up cycles from 1700UTC to 1730UTC might be also informative durations for monitoring the possibility whether or not the newly initialized model state develops into severe thunderstorms.

c) Forecast improvement by the radar reflectivity assimilation

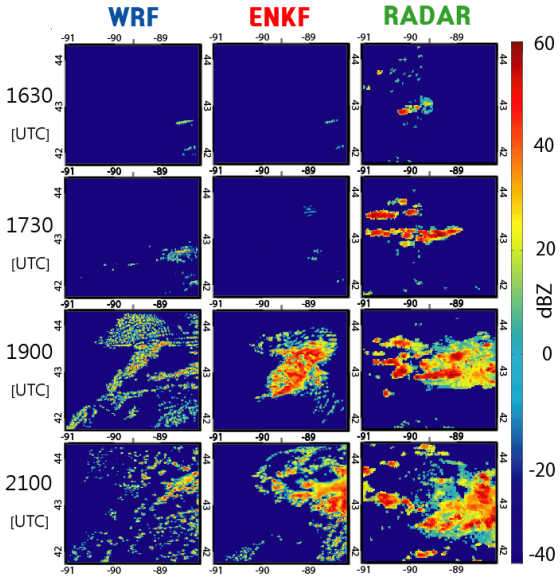

Fig. 8. Observation assimilation effect in the forecast system (Control vs. EXP.3): WRF (control without the radar assimilation), ENKF(EXP.3 with the radar assimilation based on the new method), RADAR (base radar reflectivity observation); 16:30UTC (assimilation), 17:30UTC (spin-up), 19:00UTC & 21:00UTC (forecasts)

After applying the approximate *HA* and the weighting technique introduced in the new method we can truly examine how the forecasting capability is improved by the radar reflectivity assimilation. The EXP. 3 (ENKF in Fig. 8) shows the radar data assimilation at 16:30UTC. In the Madison flood case study, 1600~1700 UTC is the most effective time for the quality control of the radar reflectivity. Because precipitation in these cycles is still distributed far from the ground cluster of the radar reflectivity around the center of the radar, the non-precipitation feature can be easily removed from the precipitation distribution. Also, if precipitation doesn't appear on the model simulation, the link between observation and model state (rescaling factor t) is absent in EnKF implementation. Therefore, at 1600UTC, the radar reflectivity observation starts being assimilated in WRF.

After assimilating the radar reflectivity, the spin-up time (1700 ~1730UTC in this study) is needed for

hydrological balance due to the disparity between the present background feature and newly introduced observational feature on model states. This process is well displayed at 1730UTC (See Fig. 8-ENKF).

The main difference between assimilation (ENKF) and non-assimilation (WRF) is most clear at 1900UTC. In this stage, the control run simulates only weak frontal precipitation (WRF in Fig. 8). Contrarily, instead of the weak and scattered convections, the ENKF forecast shows the well organized deep convection popping-up simulated high radar reflectivity. During 1900~2200 UTC, the model domain includes a whole convective cell. Therefore, the forecast results in these cycles are well matched to the real radar observation. However, after 2200 UTC the forecast results do not well correspond quantitatively to the compared radar observation, because the convective cell in the forecast model disappears crossing the boundary of the model domain earlier than radar measurement.

4) Summary and discussion

In this study it was determined that in order to utilize highly non-linear observation operator and intermittent physical properties for the data assimilation, the following conditions are necessary for the background error covariance matrix: the initial perturbation which is associated with the future targeted observation, the appropriate forecast correlation in the Kalman gain, the Gaussian distribution maintenance during sequential updates and the error renormalization for underestimated background error. All these considerations aim to design the well-conditioned and effective background error covariance matrix for the data assimilation.

We presented the following experiments systemically to solve each problem. In summary, for the fast but accurate forecast of severe convective precipitation, the radar observation and EnKF are utilized in this study, but it is quite a challenge to apply them together because of the “non-linearity” of the observation operator and the "Gaussian assumption" of EnKF. Therefore, the new method proposed in this paper, the approximation of the background error covariance matrix, is developed to linearize the Kalman gain (relative information) with the Gaussian proxy variable and, in addition, to renormalize the nonlinear and/or discontinuous observation increment (absolute information) with the weighting factor. It means that new method optimizes the linear response among the ensemble spread of the various model variables and conserves the non-linear response of the ensemble mean of the model variables to the observation increment variance.

The EnKF with the well conditioned background error covariance matrix remarkably improves the short-term forecast performance for the mesoscale convective precipitation. This result is the good initial forecast for Madison flood case in July 27 2006.

Table 2 : The summary of the problems, solutions and results on each experiment

	Control	EXP.1	EXP.2	EXP.3
HA in *K*	-	Original	Approximate	Approximate
HA–A correlation	-	Instant corr.	Forecast corr.	Forecast corr.
HA response to *A*	-	Non-linear	Linear	Linear
HA PDF	-	Non-Gaussian	Gaussian	Gaussian
Filter behavior	-	Unstable	Stable	Stable
B in *K*	-	Ill- conditioned	Well-conditioned	Well-conditioned
Weighting factor	-	f = 1.0	f = 1.0	f = 0.1
BG error in *N*	-	Unrealistic	Underestimated	Enhanced
OB error in *N*	-	Original scale	Largely developed	Diminished
Update by Obs.	-	Problematic	Insufficient	Significant
Forecast	No convection	Scattered weak convection	Shallow convection	Severe deep convection

References

Anderson, J. L. (2001). "An ensemble adjustment Kalman filter for data assimilation." Monthly Weather Review 129(12): 2884-2903.

Beezley, J. D. and J. Mandel (2008). "Morphing ensemble Kalman filters." Tellus Series a-Dynamic Meteorology and Oceanography 60(1): 131-140.

Evensen, G. (1994). "Sequential data assimilation with a nonlinear quasi-geostrophic model using Monte-Carlo methods to forecast error statistics." Journal of Geophysical Research-Oceans 99(C5): 10143-10162.

Evensen, G. (2003). "The ensemble Kalman filter: Theoretical formulation and practical implementation." Ocean Dyn. 53: 343–367.

Hamill, T. M. and J. S. Whitaker (2005). "Accounting for the error due to unresolved scales in ensemble data assimilation: A comparison of different approaches." Monthly Weather Review 133: 3132-3147.

Hong, S.-Y., Lim, J (2006). "The WRF Single-Moment 6-class Microphysics Scheme (WSM6)." J. Korean Mete Soc., 42: 129 - 151.

Houtekamer, P. L., H. L. Mitchell, et al. (2005). "Atmospheric data assimilation with an ensemble Kalman filter: Results with real observations." Monthly Weather Review 133(3): 604-620.

Kalman, R. E. (1960). "A new approach to linear filtering and prediction problems." Journal of Basic Engineering 82((1)): 35–45.

Mandel, J. (2006). "Efficient implementation of the ensemble Kalman filter." University of Colorado at Denver and Health Sciences Center CCM Report 231.

Snyder, C. and F. Q. Zhang (2003). "Assimilation of simulated Doppler radar observations with an ensemble Kalman filter." Monthly Weather Review 131(8): 1663-1677.

Sun, J. Z. (2005). "Convective-scale assimilation of radar data: Progress and challenges." Quarterly Journal of the Royal Meteorological Society 131(613): 3439-3463.

Whitaker, J. S. and T. M. Hamill (2002). "Ensemble data assimilation without perturbed observations." Monthly Weather Review 130(7): 1913-1924.

Xue, M., Y. S. Jung, et al. (2007). "Error modeling of simulated reflectivity observations for ensemble Kalman filter assimilation of convective storms." Geophysical Research Letters 34(10): 5.